



DIAGNOSTICS OF DUST PARTICLES ACCELERATION IN DUSTY PLASMA AFTERGLOW

I.I. FILATOVA^{1,c}, F.M. TRUCKACHEV²

¹Institute of Physics of NAS Belarus, Minsk, 220072, Belarus

²Department of Physical and Technical Disciplines, Mogilev State A. Kuleshov University, Mogilev, 220030, Belarus

^cCorresponding author: Tel.: +375172842346; Fax: +375172840879; Email: filatova@imaph.bas-net.by

KEYWORDS:

Main subjects: dust particle motion investigation in dusty plasma afterglow

Visualization method(s): laser sheet imaging

Other keywords: dust grain, residual charge, grain size

ABSTRACT: The dust grain dynamics in plasma of a capacitively coupled radio frequency discharge and in the post-discharge have been studied using the laser sheet imaging method. The decay of dust structures is investigated in the plasma afterglow and the numerical simulations are performed taking into account balance of forces acting on dust particles for estimation of their size and residual charge after the extinction of plasma.

INTRODUCTION

Investigations of dust-particle dynamics in dusty plasma is of great importance for solving fundamental problems in the physics of nonideal plasma and solid state [1], as well as for optimization of many industrial technologies related to surface modification, cleaning of plasmachemical devices, separation of macroparticles by size, synthesis of nanoparticles, and creation on nanostructured coatings [2–4]. Information on the dynamics of macroparticles in gas-discharge plasmas makes it possible to develop new methods of plasma diagnostics using dust grains as microprobes [5–7]. Recent studies have shown that dust grains can preserve their residual charge for several seconds after the discharge is switched off [8–12]. This phenomenon was observed both under microgravity [8] and laboratory conditions [9–11] and opens up new possibilities for dusty plasma applications.

Negatively charged dust grains in the afterglow of an RF discharge were observed in the experiments performed aboard the International Space Station [8]. In [9], diffusion of dust grains with sizes of 8–50 nm in the afterglow of an RF discharge was studied and the fraction of charged grains after switching-off of the RF power was determined. In [10], the residual charge of submicrometer-sized polymer dust grains in an RF discharge in argon was measured. The grain charge was determined by analyzing the dynamics of grain motion in a low-frequency electric field after the RF discharge was switched off. In this case, the gravity force was balanced by the thermophoretic force. It was found that, after the RF power was switched off, the grains conserved their charge for several tens of seconds, the average charge varied from $-3e$ to $-5e$, depending on the gas pressure in the discharge chamber. In [11], where the residual grain charge in the afterglow of an RF discharge was studied in more detail, it was found that, along with negatively charged grains, there were also positively charged grains and a model was proposed that explained the emergence of positively charged grains in the post-discharge phase.

Here, we present results from experimental studies of the dust grain dynamics in the afterglow of an RF discharge in air. In contrast to [10], polydisperse dust grains were injected into the discharge plasma from the outside. The experiments were performed in a discharge chamber with cooled electrodes. This made it possible to eliminate the influence of the thermophoretic force on dust grains. The dust grain dynamics after the RF power was switched off was controlled by applying an external DC electric field.

THE EXPERIMENTAL SETUP AND RESULTS

Figure 1 shows a schematic diagram of the setup for investigation of dusty plasma in an RF capacitively coupled discharge. The discharge was excited at a frequency of 5.28 MHz between two 120-mm-diameter cooled copper electrodes separated by a distance of $L = 21$ mm. The plasma-forming gas was atmospheric air at a pressure of 100 Pa. The specific input power deposited in the discharge was $W = 0.5$ W/cm⁻³. Under the experimental conditions, the



electron density and the electron and ion temperatures were $n_e \sim 10^8 \text{ cm}^3$, $T_e \sim 2 \text{ eV}$, and $T_i \sim 0.03 \text{ eV}$, respectively. Polydisperse Al_2O_3 grains with effective dimensions of $r_p \sim 0.1\text{--}20 \text{ }\mu\text{m}$ were used as dust particles.

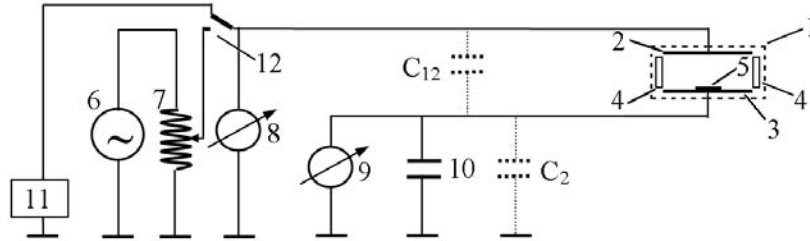


Fig. 1 Schematic diagram of the experimental setup: 1– vacuum chamber, 2 – upper electrode, 3– lower electrode, 4– quartz plates, 5– acoustic radiator with a deposited layer of dust grains, 6– RF generator; 7– inductor; 8, 9– voltmeter, 10– coupling capacitor, 11– dc power supply, 12– switch, C_{12} – capacitance between the upper and lower electrodes, and C_2 – capacitance between the lower electrode and the ground

In order to reveal the presence of a residual charge on dust grains after the discharge was switched off, a DC voltage from stabilized power supply 11 was applied through a switch 12 to the upper electrode instead of the RF voltage (Fig. 1). The value of the DC voltage was about 37 V, which corresponded to the electric field strength $E = 1760 \text{ V/m}$ between the electrodes. It was assumed that grains having a negative residual charge would shift toward the upper electrode.

Dust particles were injected into the plasma by means of a piezoelectric radiator situated on the lower electrode. Photographs of grains illuminated by a narrow laser sheet ($\lambda = 635 \text{ nm}$) with a thickness of about 1 mm and height of 20 mm in the plane perpendicular to the electrode surface were taken using a standard video camera with a frame rate of 25 s^{-1} (Fig. 2).

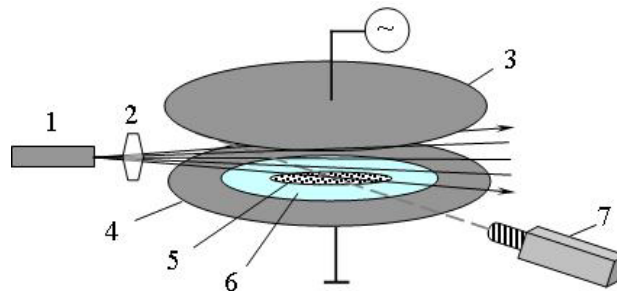


Fig. 2 Scheme of dust particle and dust structure visualization: 1– laser, 2– cylindrical lens, 3 and 4– powered and grounded electrode correspondingly, 5– particles, 6– piezoelectric radiator, 7– video camera

The recorded signal, after transforming by a Pinnacle 700 USB device, was processed by a personal computer. To minimize image distortion, the frames were stored in the Digital Video format with a resolution of 720×576 pixels, which corresponded to a spatial resolution of 0.044 mm/pixel . The velocities of grains were determined from variations in their positions estimated using a series of successive frames, which reflected the dynamics of grains over a time interval of $\Delta t \sim 0.4 \text{ s}$ after switching-off of the discharge and termination of plasma recombination. The time resolution of the video camera was 40 ms. Video images of particles were analyzed for the determination of velocities of both the dust layers and individual grains.

In order to reveal the presence of a residual charge on dust grains after the discharge was switched off, a DC voltage from stabilized power supply 11 was applied through a switch 12 to the upper electrode instead of the RF voltage (see Fig. 1). The value of the DC voltage U_{DC} was about 37 V, which corresponded to the electric field strength $E = 1760 \text{ V/m}$ between the electrodes. It was assumed that grains having a negative residual charge would shift toward the upper electrode.



It was found that the dust structure formed in the discharge plasma consisted of several layers. Dust particles levitated above the lower electrode. The levitation distance depended on the grain size. The largest grains from the lower layers precipitated onto the electrode just after the discharge was switched off. We studied the dynamics of the two upper layers (I) and (II) formed at distances of 12 and 9 mm from the lower electrode, respectively, which preserved their structure for about 1 s after the discharge was switched off (Fig. 3). In order to reveal the presence of a residual charge on dust grains, the character and velocity of grain motion in both the presence and absence of a positive potential U_{DC} on the upper electrode were analyzed.

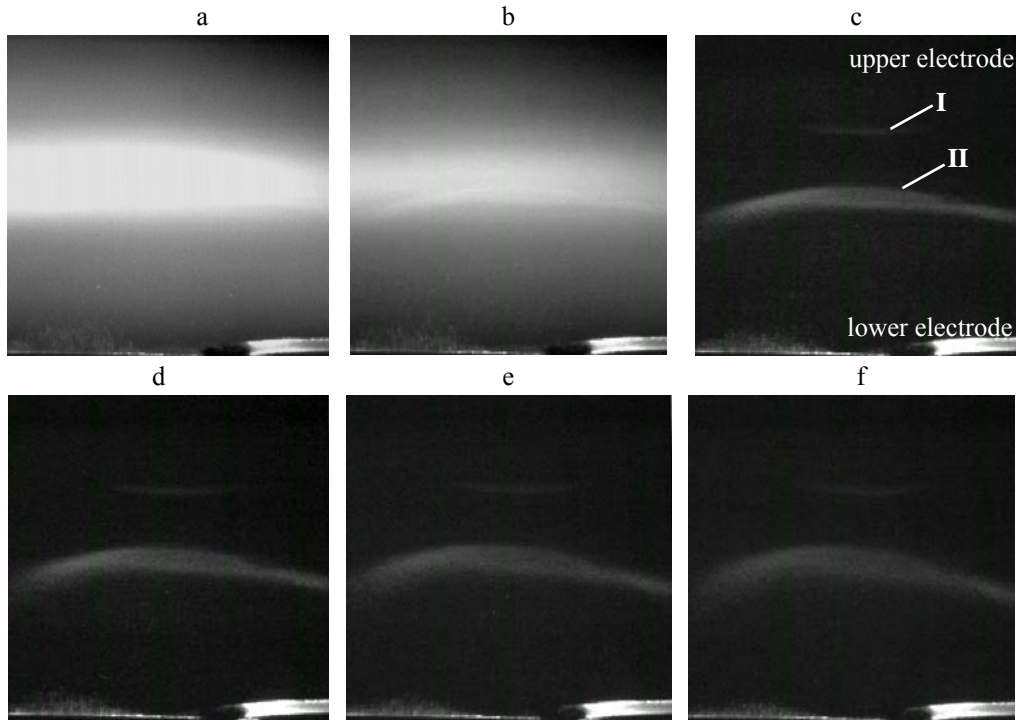


Fig. 3 The dust structure formed in plasma (a) and its decay in the afterglow: in 2 ms (b), 42 ms (c), 82 ms (d), 122 ms (e) and 162 ms (f) after the discharge switching-off

It was difficult to resolve individual grains in layer I, because their number density was too high. Hence, the grain dynamics in this layer was estimated by analyzing variations in the position of the upper boundary of the layer. For layer II, we analyzed variations in the positions of both the upper boundary of the layer and individual grains. In the absence of the potential U_{DC} , grains from layers I and II moved downward with steady-state velocities of $v_{pI} \approx 2.2$ mm/s and $v_{pII} \approx 5$ mm/s, respectively. After applying a positive potential U_{DC} , grains from both layers moved upward with the same velocities $v_{IE} = v_{IIE} \approx 2.2$ mm/s.

THEORETICAL MODEL

The size and charge of dust grains were estimated from the balance of forces acting on the grains in the post-discharge phase (Fig. 4). It was assumed that the grains were spherical. After the discharge is switched off, the grains are subject to the gravity force F_G and the neutral drag force F_{ND} [1],

$$F_G = \frac{4}{3} \pi r_p^3 \rho g, \quad (1)$$

$$F_{ND} = \frac{8}{3} \sqrt{2\pi} r_p^2 m_n n_n v_{Tn} \left(1 + \frac{\pi}{8} \right) |v_p - v_n|, \quad (2)$$

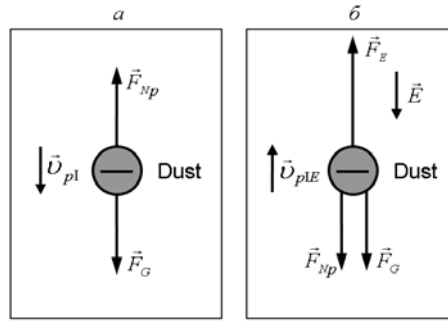


Fig. 4 Scheme of dust grain motion after the RF power is switched off (a) in the absence of an external electric field and (b) on applying a positive potential to the upper electrode

where r_p is the effective radius of dust grains; ρ is their mass density ($\rho = 2400 \text{ kg/m}^3$ for Al_2O_3); g is the free fall acceleration; m_n is the mass of a buffer gas (air) molecule; n_n is the density of buffer gas molecules; $v_{Tn} = \sqrt{8T_n / \pi m_n}$ is their thermal velocity; and v_n and v_p are the drift velocities of the buffer gas and dust grains, respectively. The mean relative molecular mass of air taking into account the percentage of its chemical components was taken equal to 29. In computations, it was assumed that $v_n = 0$. Expression (2) is valid for $K_n \gg 1$, where $K_n = l/r_p$ is the Knudsen parameter and l is the mean free path of neutral gas molecules. Under our experimental conditions, K_n was higher than 100.

The balance of vertical forces acting on grains after the discharge is switched off is described by the equation (see Fig. 4a)

$$F_G = F_{Np}. \quad (3)$$

The grain radius r_p was estimated using the following expression resulting from equations (1) – (3):

$$r_p = \frac{2m_n n_n v_{Tn} v_p}{\rho g} \sqrt{\frac{2}{\pi} \left(1 + \frac{\pi}{8}\right)}. \quad (4)$$

It was found that $r_{pI} \cong 0.1 \text{ } \mu\text{m}$ and $r_{pII} = 0.25 \text{ } \mu\text{m}$ for grains from layers I and II, respectively.

After applying a positive potential U_{DC} , in addition to the gravity force and the neutral drag force, the grains were subjected to the electric force F_E (see Fig. 4b),

$$F_E = QE, \quad (5)$$

where $Q = Ze$ is the dust grain charge, e is the elementary charge, and $E = U_{DC} / L$ is the DC bias. In this case, the balance equation takes the form

$$F_G + F_{Np} = F_E. \quad (6)$$

The residual grain charge Q was estimated by the following formula obtained with allowance for Eqs. (1), (2), (5), and (6):

$$Q = \frac{4}{3} \frac{\pi r_p^2}{E} \left(r_p \rho g + 2 \sqrt{\frac{2}{\pi}} m_n n_n v_{Tn} v_p \left(1 + \frac{\pi}{8}\right) \right). \quad (7)$$

The values of Q for grains from layers I and II were found to be $Q_I = -1e$ and $Q_{II} = -8e$, respectively. This result agrees well with the results obtained in [8, 9].

In conclusion, we consider a situation in which the sort of buffer gas is unknown and the neutral drag force F_{Np} is difficult to express explicitly (e.g., when operating with a multicomponent gas mixture or when the gas mixture composition changes due to plasmachemical reactions). In the absence of data on the buffer gas, the charge and size of



dust grains cannot be determined directly; however, the model allows one to find how the grain size is related to the grain charge, provided that the dynamics of grains in both the presence and absence of an external electric field are known. We obtained such a relationship for grains from layer II. It was assumed that the residual charge varied from one elementary charge to several tens of elementary charges [8, 9] and the neutral drag force was proportional to their velocity with respect to the neutral gas.

For grains from layer I, we obtained the following relationship:

$$|v_{pII}| = 2.3 |v_{pIE}|. \quad (8)$$

According to expression (2), the same relationship holds for the neutral drag forces F_{Np} in formulas (3) and (6), which describe the balance of forces acted on dust grains in the absence and presence of the DC bias, respectively. Then, Eq. (6) can be written in the form $1.4 \cdot F_G = F_E$. With allowance for expressions (1) and (5), the grain radius r_{pII} as a function of the residual grain charge Z can be represented as follows:

$$r_{pII} = (3ZeE / 5.8\pi\rho g)^{1/3}. \quad (9)$$

The obtained dependence is shown in Fig. 5. It is seen that the radii of grains with charges from $-1e$ до $-10e$ lie in the range $0.1 - 0.25 \mu\text{m}$, which agrees with experimentally measured values of r_p . Thus, the relationship between the charge and size of a dust grain in the discharge afterglow can be obtained using the experimental data on the character of grain motion in the external electric field. The dust particle radius as a function of the residual charge is represented in Fig. 5.

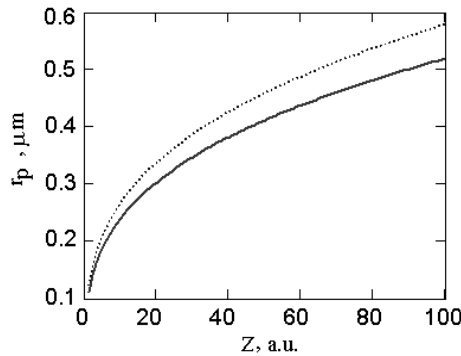


Fig. 5 Particle radius estimated in dependence on the residual charge for the layers I (solid) and II (dotted)

We could not experimentally define the concentration of dust particles n_p directly from the video images because of the insufficient resolution of a recording apparatus. In this connection, an indirect method has been proposed for the evaluation of n_p . Taking into consideration the fact that the dust cloud decays more slowly than it moves under the influence of the external forces, we suppose that the electric field E' produced by particles in the dust cloud has to be less than the external electric field E (let us assume $E' \leq E \cdot 10^{-2}$). The expression for the dust concentration in the dust cloud with the shape of a horizontal disk of radius R and thickness h , is

$$n_p = \sigma/hQ, \quad (10)$$

here, σ is the surface density of the electric charge ($\sigma = 2E'\epsilon_0$), $\epsilon_0 = 8.85 \cdot 10^{-12}$ F/m is the vacuum permittivity. With regard for the cloud size measured from the experiment ($R \approx 2.5$ mm, $h \approx 0.4$ mm), we can obtain finally the following expression for the dust concentration: $n_p = 2E'\epsilon_0/hQ$. The estimated value $n_p \leq 5 \cdot 10^5 \text{ cm}^{-3}$ for $Q = -10e$ agrees with the experimental results obtained in [13].

CONCLUSIONS

The dynamics of dust structures in the afterglow of an RF discharge in air at a pressure of 100 Pa has been investigated, and a theoretical model for estimating the size and charge of levitating grains has been proposed. It is



found that, after the RF power is switched off, dust grains with radii of $r_p = 0.1\text{--}0.25\ \mu\text{m}$ preserve a residual negative charge which value can vary in the range from $-1e$ to $-10e$, depending on the grain size. The property of dust grains to preserve their electric charge in the afterglow plasma offers new opportunities for the development of new nanotechnologies based on the possibility to control the motion of nanosized grains in the post-discharge phase by applying an external electric field.

REFERENCES

1. Shukla P. and Mamun A. *Introduction to Dusty Plasma Physics*. IOP, Bristol, 2002
2. Selwyn G. S. et al. *In situ plasma contamination measurements by He-Ne laser light scattering: A case study*. J. Vac. Sci. Technol. 1990. **A8**, p. 1726
3. Bouchoule A. *Dusty Plasmas: Physics, Chemistry and Technological Impacts in Plasma Processing*. John Wiley, New York, 1999
4. Stoffels E. et al. *Surface processes of dust particles in low pressure plasmas*. Phys. Scr. 2001. **T89**, p. 168
5. Law D.A. et al. *Dust as a Sheath Diagnostic*. Proc. of the 24th Int. Conf. on Phenomena in Ionized Gases, Warsaw, Poland, 1999, Vol. IV, p. 109
6. Swinkels G. H. P. M. et al. *Microcalorimetry of dust particles in a radio-frequency plasma*. J. Appl. Phys. 2000. **88**, p. 1747
7. Kersten H. et al. *Plasma-powder interaction: trends in applications and diagnostics*. Int. J. Mass Spectrom. 2003. **223–224**, p. 313
8. Ivlev A.V. et al. *Decharging of Complex Plasmas: First Kinetic Observations*. Phys. Rev. Lett. 2003. **90**, p. 055003
9. Childs M. A. and Gallagher A. *Plasma charge-density ratios in a dusty plasma*. J. Appl. Phys. 2000. **87**, p. 1086
10. Couëdel L. et al. *Residual dust charges in discharge afterglow*. Phys. Rev. 2006. **E 74** (2), p. 026403
11. Couëdel L. et al. Europhys. Lett. 2008. **84**, p. 35002
12. Couëdel L. *Influence of the ambipolar-to-free diffusion transition on dust particle charge in a complex plasma afterglow*. Physics of Plasmas. 2008. **15** (6), p. 063705
13. Fortov V.E. et al. *Non-ideal classical thermal plasma: experimental study of ordered structures of macroparticles*. J. Exp. Theor. Phys. 1997. **111** (2), p. 467 (in Russian)